



# Biocompatibility, Biomineralization, and Maturation of Collagen by RTR<sup>®</sup>, Bioglass and DM Bone<sup>®</sup> Materials

Francine Benetti<sup>1,2</sup>, Carlos Roberto Emerenciano Bueno<sup>2</sup>, Alexandre Henrique dos Reis-Prado<sup>1</sup>, Marina Trevelin Souza<sup>3</sup>, Juliana Goto<sup>2</sup>, Jose Maurício Paradella de Camargo<sup>2</sup>, Marco Antônio Húngaro Duarte<sup>4</sup>, Elói Dezan-Júnior<sup>2</sup>, Edgar Dutra Zanotto<sup>3</sup>, Luciano Tavares Angelo Cintra<sup>2</sup>

<sup>1</sup>Department of Restorative Dentistry, School of Dentistry, UFMG - Universidade Federal de Minas Gerais, Belo Horizonte, MG, Brazil  
<sup>2</sup>Department of Endodontics, School of Dentistry, UNESP - Universidade Estadual Paulista, Araçatuba, SP, Brazil  
<sup>3</sup>Department of Materials Engineering, Vitreous Materials Laboratory (LaMaV) UFSCar - Universidade Federal de São Carlos, SP, Brazil  
<sup>4</sup>Department of Dentistry, Endodontics and Dental Materials, School of Dentistry, USP - Universidade de São Paulo, Bauru, SP, Brazil

Correspondence: Prof. Francine Benetti, Rua Prof. Moacir Gomes de Freitas, 688, 31270-901 Belo Horizonte, MG, Brasil. Tel: +55-31-3409-2404. e-mail: francine-benetti@ufmg.br

This study evaluated the biocompatibility, biomineralization, and collagen fiber maturation induced by Resorbable Tissue Replacement (RTR<sup>®</sup>;  $\beta$ -tricalcium phosphate [TCP]), Bioglass (BIOG; bioactive glass), and DM Bone<sup>®</sup> (DMB; hydroxyapatite and  $\beta$ -TCP) in vivo. Sixty-four polyethylene tubes with or without (control group; CG) materials ( $n=8$ /group/period) were randomly implanted in the subcutaneous tissue of 16 male Wistar rats (four per rat), weighting 250 to 280 g. The rats were killed after 7 and 30 days ( $n=8$ ), and the specimens were removed for analysis of inflammation using hematoxylin-eosin; biomineralization assay using von Kossa (VK) staining and polarized light (PL); and collagen fiber maturation using picrosirius red (PSR). Nonparametric data were statistically analyzed by Kruskal-Wallis and Dunn tests, and parametric data by one-way ANOVA test ( $p<0.05$ ). At 7 days, all groups induced moderate inflammation ( $p>0.05$ ). At 30 days, there was mild inflammation in the BIOG and CG, and moderate inflammation in the RTR and DMB groups, with a significant difference between the CG and RTR ( $p<0.05$ ). The fibrous capsule was thick at 7 days and predominantly thin at 30 days in all groups. All materials exhibited structures that stained positively for VK and PL. Immature collagen fibers were predominant at 7 and 30 days in all groups ( $p>0.05$ ), although DMB exhibited more mature fibers than BIOG at 30 days ( $p<0.05$ ). RTR, BIOG, and DMB were biocompatible, inducing inflammation that reduced over time and biomineralization in the subcutaneous tissue of rats. DMB exhibited more mature collagen fibers than BIOG over a longer period.

**Key Words:** biocompatibility, bioglass, biomineralization, bone regeneration,  $\beta$ -tricalcium phosphate.

## Introduction

Although bone grafting is one of the most common surgical procedures for orthopedic treatment and rehabilitation, bone healing of critical-size defects remains a challenge in the fields of surgery, and endodontics (1). The absence of a healthy and sufficient remnant in such cases makes successful repair exceedingly difficult (2). The volume of crestal bone resorption may vary according to the reason for tooth loss (3). A systematic review reported a rapid bone loss in the first 3 to 6 months after tooth extraction in humans, reaching up 63% of horizontal bone loss in 6 months (3).

Autogenous bone is a gold standard material for reconstructive procedures of bone defects due to its potential for osteogenesis, osteoconduction, and osteoinduction (4). However, other bone substitutes or biomaterials have been investigated due to cases with insufficient bone volume and possible morbidity caused to the donor site (4). Some biocompatible materials can induce the mineralization process in tissues and, when associated with tissue engineering techniques, have yielded encouraging outcomes in terms of bone formation (2,5). Synthetic biomaterials, such as  $\beta$ -tricalcium phosphate

( $\beta$ -TCP) and bioactive glass, have been proposed as bone graft replacement materials (6,7). Although their clinical effectiveness has not yet been extensively demonstrated (3), these materials appear to exhibit high osteoconductive capacity (6).

Resorbable Tissue Replacement (RTR<sup>®</sup>; Septodont, Saint-Maur-des-Fosses, France) is a bone substitute produced using synthetic  $\beta$ -TCP granules that may be gradually absorbed by the organism (8). The granules are 500  $\mu$ m to 1 mm in size, with macropores ranging from 100  $\mu$ m to 400  $\mu$ m, and micropores  $<10$   $\mu$ m in diameter (8). Another synthetic biomaterial is Bioglass 45S5, a bioactive glass with potential for osteoconduction, osteoinduction, and high degradability (9). A previous study revealed that this bioactive glass was capable of producing a hydroxyapatite (HA) layer in test solutions that did not contain calcium or phosphate ions (10). This material demonstrated high performance in binding to hard tissues, providing support for its clinical use in procedures aimed at maintaining the alveolar ridge (11).

In the search for bone graft material(s) with osteoconduction and osteoinduction properties, the DM Bone<sup>®</sup> (MetaBiomed, Colmar, PA, USA) has been suggested

to be appropriate for bone grafting. According to the manufacturer, DM Bone is already available in three different packages, with granules ranging from 0.3~0.5 mm, 0.5~1 mm, and 1.0~2.0 mm in size (each indication will depend on the size of the surgical site/defect), composed of 60% HA and 40%  $\beta$ -TCP. However, the properties of this material have not yet been investigated.

The biocompatibility test in the subcutaneous tissue of rats is recommended by ISO for the analysis of new materials (5,12,13). Still, it is a quick test, where it is possible to compare groups with a small number of animals. Thus, the purpose of this study was to evaluate the biocompatibility, biomineralization, and maturation of collagen fibers of DM Bone® material (HA and  $\beta$ -TCP) not yet evaluated and compare them with RTR® ( $\beta$ -TCP) – both commercially available, and Bioglass 45S5 (bioactive glass used in powder form), in the connective tissue of rats. The null hypothesis was that there are no differences in biocompatibility, biomineralization, and maturation of collagen fibers among these materials.

## Material and Methods

### Animals

The study was approved by the Animal Research Ethics Committee of the local School of Dentistry (CEUA UNESP - 425-2019) and conducted according to the ARRIVE (Animal Research: Reporting of In Vivo Experiments) guidelines. Sixteen healthy male Wistar rats (*Rattus norvegicus Albinus*), weighing 250 to 280 g and 2 months old, were used. The sample size was established based on previous research (13,14). The animals were housed in polypropylene cages (four rats per cage with a height of 18 cm, depth of 41 cm, and width of 34 cm; cage bedding was changed at least three times a week) in a temperature-controlled environment (temperature,  $22 \pm 1$  °C; 70% relative humidity) with a 12 h light-dark cycle, and ad libitum access to water and food (Mogiana Alimentos SA, Campinas, Brazil). The animals were observed during the whole period of the experiment.

### Preparation of Biomaterials

RTR® (500  $\mu$ m to 1 mm in size) and DM Bone® (1 to 2 mm in size) materials' particles were gently agglutinated with distilled water, enough to moisten the material, in a sterile petri dish with the aid of a dental spatula, according to manufacturer's recommendations. Bioglass 45S5 powder (particles <5  $\mu$ m in size) was obtained from the multidisciplinary research group of the Laboratory of Vitreous Materials, at the Federal University of São Carlos, SP, Brazil. The paste was prepared by mixing the biomaterial powder with distilled water in a 2:1 (weight/weight) ratio to obtain a consistent paste. After manipulation,

biomaterials were carefully placed into polyethylene tubes using a dental spatula and vertical pluggers for RTR and DM Bone or also using a lentulo drill (Dentsply Maillefer, Tulsa, OK, USA) for Bioglass. Thus, four groups were formed according to the material: RTR®, DM Bone® (DMB), Bioglass (BIOG), and control group (CG) without material. Then, sixty-four sterile polyethylene tubes (eight per group per period) (5) (Abbott Laboratories of Brazil, São Paulo, SP, Brazil), with a 1.5-mm internal diameter and 10.0-mm length (15), were filled with materials of each group (RTR, DMB, and BIOG) until level with the end, or left empty as control (CG) (12,14,16). A sterile field was used to cover the operating bench and all instruments were also sterilized. Therefore, each animal received four polyethylene tubes: three material filled-tubes (RTR, BIOG, or DMB) and one empty tube (CG).

### Surgical Intervention

All procedures were performed in an appropriate room in the animal research area. The surgical procedure was performed according to protocols described in previous studies (5,12,14). The animals were anesthetized using ketamine 10% (80 mg/kg; Ketamine Agener 10%, União Química Farmacêutica Nacional S/A, Embu-Guaçu, SP, Brazil) and xylazine 2% (10 mg/kg; Xilazin, Syntec do Brasil LTDA, Cotia, SP, Brazil).

After shaving the rats' dorsal and decontaminating the surgical area using 5% iodine solution (Povidone-iodine, Betadine®, Stamford, CT, USA), a linear 2.0 cm incision was performed in a head-to-tail orientation using a #15 Bard-Parker blade (BD, Franklin Lakes, NJ, USA). The skin was then reflected to form two pockets on the right and two pockets on the left side of the incision. The three polyethylene tubes containing each one distinct material (RTR, DMB, and BIOG) and one empty tube (CG), were randomly distributed and positioned into the pockets. Firstly, the positions of the four tubes (one each group) in the first animal were defined by the lottery. In the next animal, the clockwise rotation was adopted for the next tubes. This method was used for all animals. At the end of the surgical procedures, the same number of the tubes per group was allocated to each animal's dorsal region. The site was identified according to the material received, and it was closed using 4-0 silk sutures.

### Tissue Processing and Histological Analysis

After 7 and 30 days, the animals (n=8 each period) were killed using an overdose of anesthetic solution. The implanted tubes, along with the surrounding tissues, were removed and fixed in 10% formalin solution (Dinâmica Química Contemporânea LTDA, Indaiatuba, SP, Brazil) at a pH of 7.0. Then, the specimens were sectioned in half to

remove tubes from inside the fixed tissue, and the tissue that was around one extremity was randomly selected for processing (13,16). The specimens were submitted to routine laboratory processing and embedded in paraffin. The paraffin blocks were oriented parallel to the long axis of the tubes, and longitudinal and semi-serial histological cuts (5  $\mu$ m or 10  $\mu$ m thick) were obtained from the central areas of the implants. Histological sections (5  $\mu$ m) were prepared for hematoxylin-eosin (HE) and picosirius red (PSR) staining, while the 10  $\mu$ m histological sections were prepared for staining according to the von Kossa (VK) technique or kept unstained for polarized light (PL) examination (14).

A single calibrated operator from previous studies (5,13,14) performed all analyses in a blinded manner under light microscopy (DM 4000 B, Leica Microsystems, Wetzlar, Germany) using 100 $\times$  (VK and PL examination) and 400 $\times$  magnification (HE and PSR staining) (16). The intensity of the inflammatory reaction in tissues in close contact with the materials in the tubes was scored as follows (5,13): 1, none or few inflammatory cells and no reaction; 2, <25 cells and mild reaction; 3, between 25 and 125 cells and moderate reaction; and 4,  $\geq$ 125 cells and severe reaction. For this analysis, the number of cells for each group was obtained by the optical field from the center of the tube opening region (400 $\times$  magnification) (14,16). Two histological sections of the one blade of each specimen were evaluated to determine the score of inflammation, and the operator would consensus if there were any differences. The thickness of fibrous capsules was calculated in these same two histological sections and the average was obtained. Then, the fibrous capsules were classified as thin when <150  $\mu$ m and thick when  $\geq$ 150  $\mu$ m (5,12). The maturation levels of the collagen fibers were assessed in sections stained with PSR under polarized light microscopy. Similarly, this analysis was also performed in two consecutive histological

sections of the same blade, and the average value for each type of fiber of the specimen was considered for analysis. Greenish-yellow fibers were considered to be immature and thin, while yellowish-red fibers were classified as mature and thick (17). After color selection, the software automatically calculated the marked area of each collagen fiber type (Leica QWin V3, Leica Microsystems). The VK-positive structures or birefringent structures under PL were recorded as either present or absent (5,14).

### Statistical Analysis

The normal distribution of data was confirmed by the Shapiro-Wilk test. After, the parametric data (PSR at 7 days) were analyzed by a one-way analysis of variance (ANOVA), followed by Tukey post-hoc test. Nonparametric data (PSR at 30 days and hematoxylin-eosin) were analyzed using the Kruskal-Wallis test, followed by the Dunn test. The *p*-value was considered significant at 5%.

## Results

The results of the histological analysis are summarized in Table 1, and representative images are shown in Figure 1. There was no loss of animals in this study. Rats were healthy on days when the tubes were removed for further processing and histological analysis.

At 7 days after tube implantation, most of the specimens the CG and BIOG exhibited moderate inflammatory infiltration, mainly of polymorphonuclear cells, such as neutrophils, throughout the fibrous capsule, but mainly in the region of the tissue that was in contact with the material. Macrophages and multinucleated giant cells were also observed. Similarly occurred to RTR and DMB; however, at least two-to-three specimens of these groups showed a severe inflammatory reaction. Furthermore, a thick and disorganized fibrous capsule in the tube opening region was observed among the groups. However, there was no significant difference among the groups (*p*>0.05).

On day 30, most specimens from the CG and BIOG groups exhibited mild inflammation, while moderate inflammation was predominant in the RTR and DMB groups. At this period, a predominant chronic inflammatory reaction composed by some lymphocytes, macrophages, and neutrophils cells, was observed in the groups, mainly in the RTR and DMB. A significant difference was observed between the RTR and CG (*p*<0.05). At this point, fibroblasts from all groups formed a thin and well-structured

Table 1. Inflammatory score, thickness of fibrous capsule and biomineralization ability according to group, at 7 and 30 days (n=8 per period)

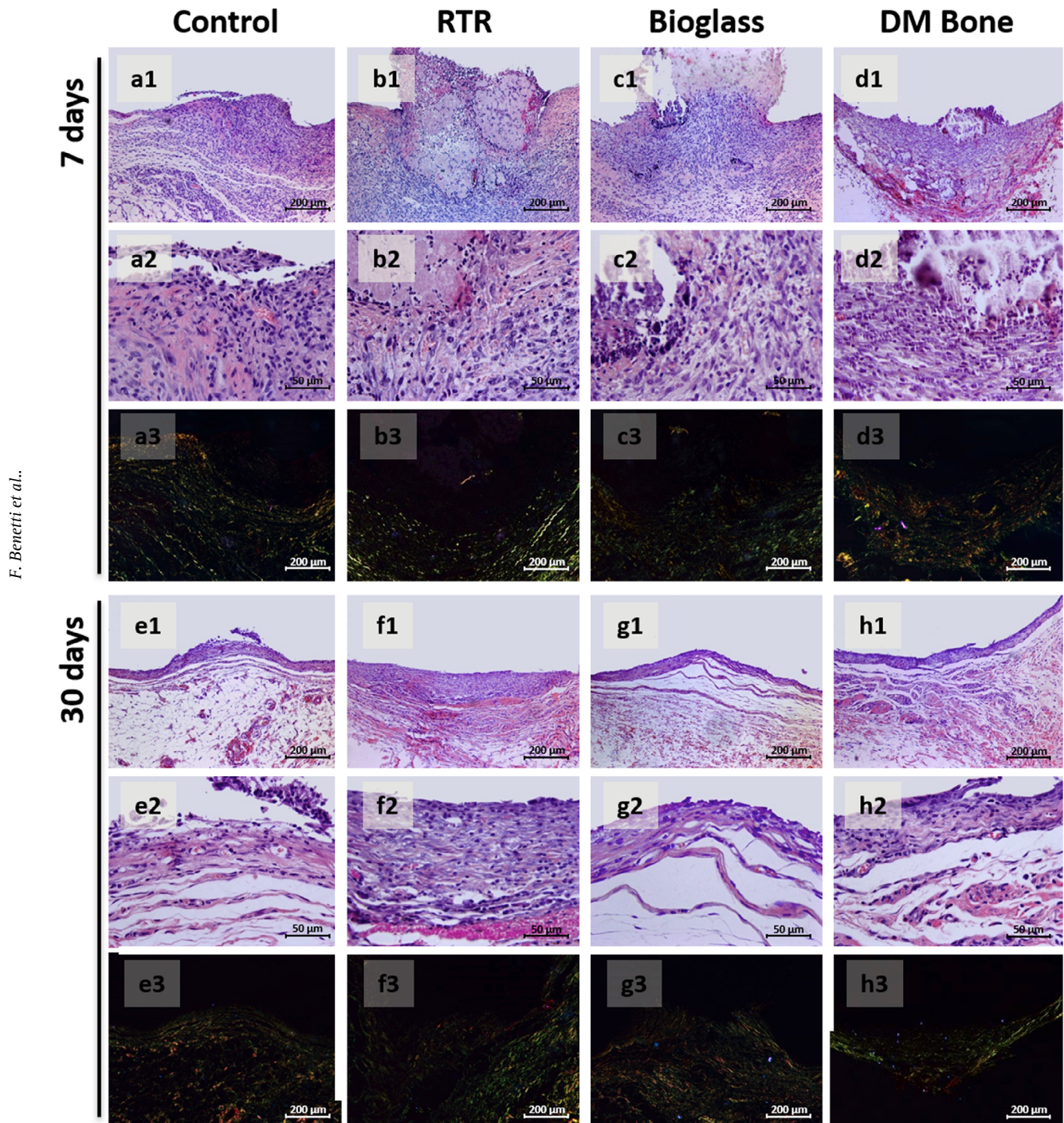
Time / p value	Groups*	Scores				Median	Capsule		Von Kossa (%)	Polarized light (%)
		1	2	3	4		Thick	Thin		
7 days p=0.229	Control <sup>a</sup>	0	2	5	1	3	8	0	0	0
	RTR <sup>a</sup>	0	0	6	2	3	8	0	100	100
	Bioglass <sup>a</sup>	0	2	5	1	3	8	0	100	100
	DM Bone <sup>a</sup>	0	1	4	3	3	8	0	100	100
30 days p=0.008	Control <sup>a</sup>	1	7	0	0	2	0	8	0	0
	RTR <sup>a</sup>	0	2	5	1	3	3	5	100	100
	Bioglass <sup>a</sup>	1	5	2	0	2	0	8	100	100
	DM Bone <sup>a</sup>	0	3	4	1	3	1	7	100	100

\*Kruskal-Wallis test followed by Dunn's test; same letters indicate no statistically significant difference among the groups in each analysis period (*p*>0.05).

fibrous capsule in all specimens from CG and BIOG, and for most specimens from the RTR and DMB.

Data pertaining to the maturation of collagen fibers

are summarized in Table 2, and representative images are shown in Figure 1. Immature collagen fibers were predominant in all groups at both time points (i.e., at 7



F. Benetti et al.

Figure 1. Representative images of the biocompatibility and collagen fibers maturation. (a1,a2 - d1,d2) At 7 days: (a1,a2) control group showed moderate inflammatory cell infiltration, (b1,b2) RTR group with the presence of severe inflammatory response, (c1,c2) Bioglass had moderate inflammatory infiltrate and (d1,d2) DM Bone had severe inflammatory response (e1,e2 - h1,h2) At 30 days: (e1,e2) control group had mild inflammatory response, (f1,f2) RTR group showed moderate inflammatory infiltrate, (g1,g2) Bioglass had mild inflammatory response and (h1,h2) DM Bone with the presence of mild inflammatory cell infiltration. (a3-h3) Collagen fibers maturation at (a3-d3) 7 days and at (e3-h3) 30 days, with higher amount of immature collagen fibers in all groups. [100x, 400x, HE; 100x, PSR].

and 30 days), and no significant difference was observed at 7 days ( $p>0.05$ ). At 30 days, the DMB had a greater number of mature collagen fibers than the BIOG ( $p<0.05$ );

there was no significant difference among the other groups ( $p>0.05$ ).

At 7 and 30 days, all experimental materials exhibited positivity for VK staining and were birefringent to PL. Areas of dystrophic calcification were observed near the tube opening or scattered in the connective tissue of the fibrous capsule. In CG, no VK positivity or birefringent structures were observed at both time points (Table 1). Representative images of biomineralization are shown in Figure 2.

Table 2. Percentages of immature and mature collagen fibers in the fibrous capsule according to group, at 7 and 30 days (n=8 per period)

Groups	7 days*		30 days*	
	Immature	Mature	Immature	Mature
Cont <sup>Aab</sup>	83.39 ± 9.81	16.61 ± 9.81	88.33 ± 2.16	11.67 ± 2.16
RTR <sup>Aab</sup>	88.16 ± 6.95	11.84 ± 6.95	81.10 ± 18.84	18.90 ± 18.84
Bioglass <sup>Aa</sup>	87.42 ± 8.61	12.58 ± 8.61	91.49 ± 4.70	8.51 ± 4.70
DM Bone <sup>Ab</sup>	87.36 ± 7.17	12.64 ± 7.17	71.86 ± 5.33	28.14 ± 5.33
P value	=0.651		=0.007	

\*One-Way ANOVA test followed by Tukey test, after normality test. ≠Kruskal-Wallis test followed by Dunn's test, after normality test. \*,#Same uppercase and lowercase letters indicate no statistically significant difference among the groups at 7 and 30 days, respectively ( $p>0.05$ ).

## Discussion

In the present investigation,

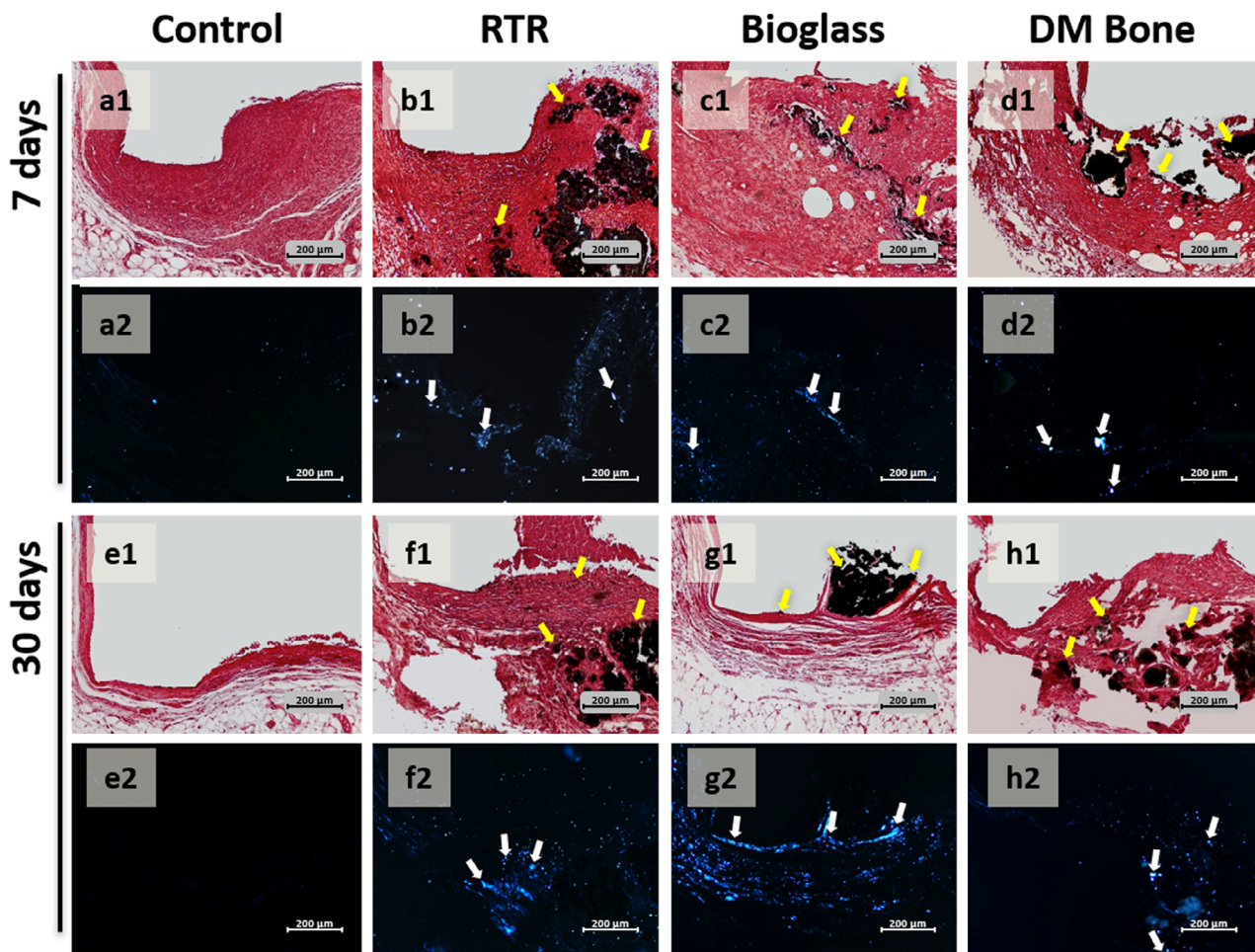


Figure 2. Representative images of biomineralization. Yellow arrows indicate VK-positive structures and white arrows indicate birefringent structures under PL. At (a1,a2-d1,d2) 7 and (e1,e2-h1,h2) 30 days. (a1,a2,e1,e2) Control group with no positive structures for von Kossa or birefringent under polarized light, and (b1,b2,f1,f2) RTR, (c1,c2,g1,g2) Bioglass, and (d1,d2,h1,h2) DM Bone groups with positive structures for von Kossa or birefringent under polarized light. [100x, VK; 100x, PL].

biocompatibility, biomineralization, and maturation of collagen fibers of three bone graft materials were evaluated. The study demonstrated that all materials were biocompatible and induced biomineralization. A greater number of immature collagen fibers were found at both time points in all groups, with a significant difference between BIOG (with more immature fibers) and DMB group only at 30 days. Thus, the null hypothesis of the study was partially accepted.

Several *in vivo* studies have investigated the inflammatory response to  $\beta$ -TCP bone substitute materials. For this analysis in this study, polyethylene tubes – which do not induce inflammation – filled with the materials were implanted into the subcutaneous tissue of rats, as a method recommended by ISO 10993-6 (12). Significant biocompatibility of this material has been reported in bone tissue (18,19), given that no detectable signs of severe inflammatory infiltrate were observed in a bone defect model in dogs (20). However, the results of the present study demonstrated an inflammatory response to  $\beta$ -TCP materials in a subcutaneous implantation model. This inflammatory response occurs after the implantation of a material in a tissue, and it has an important role in material degradation and vascularization of the implant bed (18). The insertion of the biomaterial induces the release of plasmatic and tissue proteins, and it attracts inflammatory cells, such as macrophages, to the region (7). Thus, it is not unusual to observe inflammatory infiltrate during the healing process in the area in contact with biomaterials (21).

Biocompatibility is related to the ability of a material(s) to reduce inflammation to insignificant levels over time (5), as observed. However, in similar previous studies, no inflammation was observed at each time point in subcutaneous tissue for  $\beta$ -TCP materials (18). These distinct findings may be a result of different material features used in other studies, such as granule size, shape, porosity, and surface chemistry (18).

In this study, a consistent paste derived from bioactive glass powder with particle size  $<5 \mu\text{m}$  diameter was used. These particles were smaller than those previously evaluated (180 to 212  $\mu\text{m}$  and  $\geq 40 \mu\text{m}$ ) (7,22). This mixing demonstrated biocompatibility with an evident decrease in inflammation from 7 to 30 days. This finding was consistent with other *in vivo* models, in which histological assessment of Bioglass 45S5 in fiber form (melt-derived system, 15  $\mu\text{m}$  diameter) and a variation of Bioglass 45S5 in powder form (particle size, 40  $\mu\text{m}$  to 63  $\mu\text{m}$ ), indicated the absence of necrosis and a lack of inflammatory infiltrate (22). Similarly, in another rat subcutaneous model, the incorporation of composites in bioactive glass (pore size range 50–500  $\mu\text{m}$ ) exhibited a gradual reduction in inflammatory reaction over implantation time (23). Thus, Bioglass was biocompatible

in these studies, regardless of particle size.

An earlier investigation found multinucleated giant cells (MNGCs) and leukocytes concentrated close to the particulate material of HA and TCP when evaluated at 21 days in bone tissue from rat's calvaria defects (7). At 45 days, a process of healing with a few leukocytes and elongated MNGCs were described; however, MNGCs were significantly increased in the HA/TCP group compared with the bioactive glass-ceramic group. A difference in inflammation was not observed in this present study and, again, the difference in the size of the HA/TCP particles may have influenced these results. We used particles with a diameter of 1 to 2 mm, while the previous study used particles 0.5 to 1 mm in diameter. Moreover, the use of different tissues in both studies must be considered.

At 30 days, all experimental materials induced mild to moderate inflammatory responses, and the fibrous capsule was thin. These observations were associated with well-organized tissue structure formation and collagen deposition (13).

The biomineralization ability of the bone graft materials was observed by the presence of structures birefringent to PL and positive for VK staining. The observation of these structures was related to the formation of calcite crystals in the surrounding area, originating from the reaction of calcium ions from the materials with carbonic gas from the tissue (14). Calcite crystals can participate in the initiation of biomineralization activity with proteins of the extracellular matrix, which may stimulate bone defects closure. These structures were detected in the fibrous capsule site that was in contact with all the evaluated materials. These results corroborate those of other investigations that demonstrated the potential of  $\beta$ -TCP materials in producing a significant volume of mineralized tissue associated with the formation of bone tissue (8). Studies have shown that Bioglass, which is mainly composed of silica mixed with calcium and phosphorous (1,11), exhibits osteoconductive and osteoinductive properties using the sol-gel method and/or melt-derived form (9). Likewise, Bioglass has the ability to release ions during its degradation that stimulate bone cells to promote bone regeneration (7,12). The present study demonstrated that fine particles in consistent paste form also induced biomineralization, which has not been previously described. In addition, the presence of mineralization particles in connective tissue reinforces the intense bioactivity of the evaluated materials.

Regarding DM Bone<sup>®</sup>, a recent investigation reported a material that has the similar composition (60% HA and 40%  $\beta$ -TCP), could promote the release of ions, such as  $\text{Ca}^{2+}$ , in the surrounding tissues during material degradation (7). These ions stimulated cell differentiation and organic matrix mineralization, and this process varied according

to the ratio of HA and  $\beta$ -TCP in the material (7). Higher concentrations of HA (>75%) block osteoclast activity, while higher concentrations of  $\beta$ -TCP increase biomaterial degradation (24). Therefore, physicochemical studies may find differences in the performance of RTR® and DM Bone® materials and, thus, warrant further evaluation. However, these materials did not demonstrate different results histologically.

Concomitant analysis of immature and mature collagen was performed. The PSR staining method differentiates collagen types using polarized light microscopy. Bone tissue quality may not be limited to its mineralized architecture, but also to its collagenous content as a relevant scaffold for the mineralization of bone matrix and its mechanical characteristics (7). A greenish-yellow color suggests that collagen is immature and thin. On the other hand, a yellowish-red color suggests better maturity and thick fiber organization (7,17). Considering this, in most specimens from all tested groups, immature collagen fibers were predominant. Material-induced biomineralization may have influenced the maturation of collagen fibers. This is satisfactory for a mineralization matrix and for the remodeling process because the presence of these greenish fibers favors the dynamics of the bone remodeling process by bone graft materials (7). However, a limitation of this study is that it did not evaluate the response of materials in bone tissue, where collagen may act differently.

At 30 days, DM Bone® exhibited a greater number of mature and thicker collagen fibers than Bioglass. Similar findings have been previously described, in which bioactive glass-ceramic, a parent glass of Bioglass 45S5, demonstrated significantly lower expression of mature fibers compared with HA/TCP material at day 45 (7). Thus, it may be that Bioglass has a significant potential for biomineralization in bone tissue, although both materials demonstrate this ability. We found the induction of mineralization in connective tissue for both groups. Additionally, an evaluation of the outcomes in bone tissue is necessary because of the influence of collagen fibers on these results. Nevertheless, it is known that particles of smaller sizes have a pH much higher than that for coarser particles (25), and it is suggested to analyze the new DM Bone material with smaller particle sizes.

In summary, the results of this study demonstrated that the new material, DM Bone®, elicits a tissue response similar to RTR®, which has previously been extensively studied. Furthermore, the results revealed that Bioglass in paste form is also biocompatible and induces biomineralization. All materials exhibited a significant number of immature collagen fibers than mature fibers, which may have been due to biomineralization. However, future studies investigating DM Bone® should consider other particle sizes, analyses of

different tissues, and experimental models, such as bone defects repair study, due to its potential to be used as a bone substitute. In conclusion, RTR®, Bioglass, and DM Bone® were biocompatible and induced biomineralization in the subcutaneous tissue of rats.

## Resumo

Este estudo avaliou a biocompatibilidade, biomineralização e maturação das fibras de colágeno induzidas por Resorbable Tissue Replacement (RTR®; fosfato  $\beta$ -tricalcico [TCP]), Bioglass (BIOG; vidro bioativo) e DM Bone® (DMB; hidroxiapatita e  $\beta$ -TCP) in vivo. Sessenta e quatro tubos de polietileno com ou sem (grupo controle; GC) os materiais (n=8/grupo/período) foram implantados aleatoriamente em tecido subcutâneo de 16 ratos machos Wistar (quatro por rato), pesando entre 250 a 280g. Os ratos foram mortos após 7 e 30 dias (n=8), e as amostras foram removidas para análise da inflamação utilizando hematoxilina-eosina; avaliação da biomineralização utilizando coloração de von Kossa (VK) e luz polarizada (LP); e maturação das fibras colágenas, utilizando picrosirius red (PSR). Os dados não-paramétricos foram analisados pelos testes de Kruskal-Wallis e Dunn, e os paramétricos pelo teste de one-way ANOVA (p<0.05). Aos 7 dias, todos os grupos induziram inflamação moderada (p>0,05). Aos 30 dias, houve inflamação leve nos grupos BIOG e GC, e inflamação moderada nos grupos RTR e DMB, com diferença significativa entre os GC e RTR (p<0,05). A cápsula fibrosa foi espessa aos 7 dias, e predominantemente fina aos 30 dias em todos os grupos. Todos os materiais exibiram estruturas positivas para VK e LP. Fibras colágenas imaturas foram predominantes aos 7 e 30 dias em todos os grupos (p>0,05), embora o DMB exibiu fibras mais maduras do que o BIOG aos 30 dias (p<0,05). RTR, BIOG e DMB foram biocompatíveis, induzindo inflamação que reduziu com o tempo, e biomineralização no tecido subcutâneo de ratos. O DMB exibiu mais fibras colágenas maduras do que o BIOG em período mais longo.

## Acknowledgements

This study was supported by a grant (436122/2018-9; research assistance) from the Conselho Nacional de Desenvolvimento Científico e Tecnológico – CNPq, São Paulo, SP, Brazil and by Pró-Reitoria de Pesquisa from Universidade Federal de Minas Gerais (UFMG), Belo Horizonte, MG, Brazil.

## References

1. Wang W, Yeung KW. Bone grafts and biomaterials substitutes for bone defect repair: A review. *Bioact Mater* 2017;2:224-247.
2. Bernabé PFE, Melo LGN, Cintra LT, Gomes-Filho JE, Dezan Jr E, Nagata MJ. Bone healing in critical-size defects treated with either bone graft, membrane, or a combination of both materials: a histological and histometric study in rat tibiae. *Clin Oral Implants Res* 2012;23:384-388.
3. Tan WL, Wong TL, Wong MC, Lang NP. A systematic review of post-extraction alveolar hard and soft tissue dimensional changes in humans. *Clin Oral Implants Res* 2012;23:1-21.
4. Hirota M, Matsui Y, Mizuki N, Kishi T, Watanuki K, Ozawa T, et al. Combination with allogenic bone reduces early absorption of beta-tricalcium phosphate (beta-TCP) and enhances the role as a bone regeneration scaffold. *Experimental animal study in rat mandibular bone defects*. *Dent Mater J* 2009;28:153-161.
5. Cintra LTA, Benetti F, de Azevedo Queiroz ÍO, de Araujo Lopes JM, Penha de Oliveira SH, Sivieri Araujo G, et al. Cytotoxicity, Biocompatibility, and Biomineralization of the New High-plasticity MTA Material. *J Endod* 2017;43:774-778.
6. Piattelli A, Scarano A, Piattelli M, Coraggio F, Matarasso S. Bone regeneration using Bioglass: an experimental study in rabbit tibia. *J Oral Implantol* 2000;26:257-261.
7. Munerato MS, Bigueti CC, Parra da Silva RB, Rodrigues da Silva AC, Zucon Bacelar AC, Lima da Silva J, et al. Inflammatory response and

- macrophage polarization using different physicochemical biomaterials for oral and maxillofacial reconstruction. *Mater Sci Eng C Mater Biol Appl* 2020;107:110229.
8. Pinipe J, Mandalapu NB, Manchala SR, Mannem S, Gottumukkala NVSS, Koneru S. Comparative evaluation of clinical efficacy of  $\beta$ -tri calcium phosphate (Septodont-RTR)<sup>™</sup> alone and in combination with platelet rich plasma for treatment of intrabony defects in chronic periodontitis. *J Indian Soc Periodontol* 2014;18:346-351.
  9. Wang S, Hu Q, Gao X, Dong Y. Characteristics and Effects on Dental Pulp Cells of a Polycaprolactone/Submicron Bioactive Glass Composite Scaffold. *J Endod* 2016;42:1070-1075.
  10. Hench LL, Splinter RJ, Allen WC, Greenlee TK. Bonding mechanisms at the interface of ceramic prosthetic materials. *J Biomed Mater Res* 1971;5:117-141.
  11. Hench LL. The story of Bioglass. *J Mater Sci Mater Med* 2006;17:967-978.
  12. International Organization for Standardization. ISO 10993-6: Biological Evaluation of Medical Devices Part 6: Testes for Local Effects after Implantation. Geneva:ISO;2016.
  13. Cintra LTA, Benetti F, de Azevedo Queiroz ÍO, Ferreira LL, Massunari L, Bueno CRE, et al. Evaluation of the cytotoxicity and biocompatibility of new resin epoxy-based endodontic sealer containing calcium hydroxide. *J Endod* 2017;43:2088-2092.
  14. Benetti F, de Azevedo Queiroz ÍO, Cosme-Silva L, Conti LC, Oliveira SHP, Cintra LTA. Cytotoxicity, Biocompatibility and Biomineralization of a New Ready-for-Use Bioceramic Repair Material. *Braz Dent J* 2019;30:325-332.
  15. Garcia LDA, Huck C, Menezes de Oliveira L, de Souza PP, de Souza Costa CA. Biocompatibility of new calcium aluminate cement: tissue reaction and expression of inflammatory mediators and cytokines. *J Endod* 2014;40:2024-2029.
  16. Bueno CRE, Vasques AMV, Cury MTS, Siviere-Araújo G, Jacinto RC, Gomes-Filho JE, et al. Biocompatibility and biomineralization assessment of mineral trioxide aggregate flow. *Clin Oral Investig* 2019;23:169-177.
  17. Cintra, LTA, Ferreira LL, Benetti F, Gastelum AA, Gomes-Filho JE, Ervolino E, et al. The effect of dental bleaching on pulpal tissue response in a diabetic animal model. *Int Endod J* 2017;50:790-798.
  18. Ghanaati S, Barbeck M, Orth C, Willershausen I, Thimm BW, Hoffmann C, et al. Influence of  $\beta$ -tricalcium phosphate granule size and morphology on tissue reaction in vivo. *Acta Biomater* 2010;6:4476-4487.
  19. Dulany K, Hepburn K, Goins A, Allen JB. In-Vitro and In-Vivo Biocompatibility Assessment of Free Radical Scavenging Nanocomposite Scaffolds for Bone Tissue Regeneration. *J Biomed Mater Res A* 2019;108:301-315.
  20. Tanuma Y, Matsui K, Kawai T, Matsui A, Suzuki O, Kamakura S, et al. Comparison of bone regeneration between octacalcium phosphate/collagen composite and  $\beta$ -tricalcium phosphate in canine calvarial defect. *Oral Surg Oral Med Oral Pathol Oral Radiol* 2013;115:9-17.
  21. Araujo MG, Liljenberg B, Lindhe J. Dynamics of Bio-Oss Collagen incorporation in fresh extraction wounds: an experimental study in the dog. *Clin Oral Implants Res* 2010;21:55-64.
  22. Souza LPL, Lopes JH, Ferreira FV, Martin RA, Bertran CA, Camilli JA. Evaluation of effectiveness of 45S5 bioglass doped with niobium for repairing critical-sized bone defect in in vitro and in vivo models. *J Biomed Mater Res A* 2020;108:446-457.
  23. Cui N, Qian J, Wang J, Ji C, Xu W, Wang H. Preparation, physicochemical properties and biocompatibility of PBLG/PLGA/bioglass composite scaffolds. *Mater Sci Eng C Mater Biol Appl* 2017;71:118-124.
  24. Yamada S, Heymann D, Bouler JM, Daculsi G. Osteoclastic resorption of calcium phosphate ceramics with different hydroxyapatite/beta-tricalcium phosphate ratios. *Biomaterials* 1997;18:1037-1041.
  25. Zhang D, Hupa M, Hupa L. In Situ pH within Particle Beds of Bioactive Glasses. *Acta Biomater* 2008;4:1498-1505.

Received May 12, 2020  
Accepted August 25, 2020